10.1109/ULTSYM.2009.0481

Estimation of Ultrasound Tissue Attenuation Along the Propagation Path by Applying Multiple Filters to the Backscattered Echoes

Timothy A. Bigelow, Member, IEEE
Department of Electrical and Computer Engineering
Department of Mechanical Engineering
Iowa State University
Ames, IA, USA
bigelow@iastate.edu

***Abstract*—Quantifying the correlation length of the tissue microstructure has shown potential for diagnosing between benign and malignant tumors. In order to implement these advances in the clinic, the total frequency dependent attenuation along the propagation path must be determined on a patient specific basis. Previously, an algorithm was developed to estimate this attenuation using echoes from multiple sources. In this study, the developed algorithm was extended to echoes from a single source by filtering the echoed signal into multiple frequency bands. This step was needed because it would be challenging to scan exactly the same tissue region using multiple sources in the clinic. Computer simulations were conducted to verify the attenuation could be determined by filtering the echoes from a single source. The simulations utilized a spherically focused single element source (5 cm focal length, f/4, 14 MHz center frequency, 50% bandwidth) exposing a homogeneous tissue region. The simulated tissue had Gaussian scattering structures with effective radii of 5 to 55 μm (one size per simulated case) placed at a density of 250/mm^3 (~5 scatterers/resolution cell for 14 MHz transducer). The attenuation of the tissue was also varied from 0.1 to 0.9 dB/cm-MHz. The simulations explored the dependence on scatterer size, attenuation, and region of interest (ROI) size. The computer simulations confirmed that the total attenuation along the propagation path can be determined by appropriately applying multiple filters to the backscattered echoes from a single source.**

Keywords-ultrasound tissue characterization, attenuation estimation, correlation length.

I. INTRODUCTION

Quantifying the tissue microstructure scattering correlation length by processing ultrasound echoes from tissue regions of interest has shown potential for improving many areas of diagnostic ultrasound [1-7]. When quantifying the tissue microstructure, the backscattered power spectrum from the tissue region of interest (ROI) is first compared to the backscattered power spectrum of a known target in order remove the transmission/filtering characteristics of the ultrasound source. Then, the impact of the frequency dependent attenuation along the propagation path leading up to the ROI is removed leaving only the backscatter coefficient as a function of frequency. The backscatter coefficient can then be compared to an assumed model for the tissue scattering yielding an effective scatterer diameter and acoustic concentration which can be used to quantify the scattering within a particular region. If the attenuation along the propagation path is not correctly included, then the backscatter coefficients and subsequent estimates of scatterer diameter and acoustic concentration are meaningless. Therefore, in order to quantify the tissue microstructure, the total frequency dependent attenuation along the propagation path must be accurately determined. Determination of the total attenuation is difficult due to both attenuation and scatterer correlation length modifying the backscattered power spectrum [3, 8].

Previously many different approaches have been utilized to determine the attenuation along the propagation path. Some have restricted their analysis to time domain methods by quantifying only the change in backscatter with propagation depth [9, 10], but these approaches assume that the tissue is homogeneous whereas real tissue is largely inhomogeneous. Others have attempted to estimate the total attenuation by first decomposing the tissue into smaller homogeneous regions, estimating the local attenuation within each region, and then summing these attenuations weighted by the length of each homogeneous region to obtain an estimate of the total attenuation [11, 12]. Unfortunately, summing estimates of the local attenuation is challenging due to the large, locally homogeneous region sizes needed to accurately estimate the local attenuation (~30 to 50λ) [13, 14]. Furthermore, the process is highly computationally intensive and prone to errors as the errors can accumulate with increasing propagation depth. Another approach, termed the Spectral Fit Algorithm, that has been attempted involves simultaneously estimating both scatterer correlation length and total attenuation from backscattered ultrasound echoes [8, 15, 16], but this approach is highly dependent on having the correct model for tissue scattering.

Recently, a new algorithm was developed that estimated the total attenuation along the propagation path by processing echoes from multiple sources used to scan the same tissue region [17]. The algorithm only needed echoes from a single

Supported by NIH Grant CA111289 and Iowa State University.

ROI to obtain an estimate of the total attenuation between the source and the ROI even though the algorithm did not assume that the tissue was homogeneous between the source and the ROI. Furthermore, the algorithm was only weakly dependent on the scattering properties of the tissue making it much more robust than the Spectral Fit Algorithm. However, the new algorithm could still be improved. Namely, the algorithm required multiple ultrasound sources limiting its future clinical utility since it would be challenging to scan the same tissue region with multiple ultrasound sources. In this work, the algorithm was derived for implementation using multiple filters applied to echoes from a single source. The performance of the algorithm was then verified in computer simulations.

II. Derivation of Algorithm

After applying a Gaussian filter and correcting for local attenuation and diffraction effects in the scattering region, the backscattered power spectrum from the tissue is given by,

$$\mathrm{E}\left[\left|V_{scat}(f)\right|^2\right]_{Filtered} \propto e^{\left(-\frac{\left(f-\tilde{f}_o''\right)^2}{2\tilde{\sigma}_\omega^2}\right)} e^{\left(-\frac{(f-f_c)^2}{2\sigma_c^2}\right)} \qquad (1)$$

where f_c and σ_c^2 correspond to the center frequency and bandwidth of the filter while $\tilde{f}_o''$ and $\tilde{\sigma}_\omega^2$ are the spectral peak frequency and bandwidth for the echoes returned from the tissue. Equation (1) can be simplified to yield

$$\mathrm{E}\left[\left|V_{scat}(f)\right|^2\right]_{Filtered} \propto e^{\left(-\frac{\left(f-\tilde{f}_{oc}''\right)^2}{2\tilde{\sigma}_{\omega c}^2}\right)} \qquad (2)$$

where

$$\tilde{\sigma}_{\omega c}^2 = \frac{\sigma_c^2}{\left(1+\frac{\sigma_c^2}{\tilde{\sigma}_\omega^2}\right)} \quad \tilde{f}_{oc}'' = \frac{\left(f_c + \frac{\sigma_c^2 \tilde{f}_o''}{\tilde{\sigma}_\omega^2}\right)}{\left(1+\frac{\sigma_c^2}{\tilde{\sigma}_\omega^2}\right)}. \qquad (3)$$

Similarly, if we apply a Gaussian filter to the power spectrum returned from a rigid plane (i.e., a reference spectrum) we obtain

$$\mathrm{E}\left[\left|V_{ref}(f)\right|^2\right]_{Ref\_Filtered} \propto e^{\left(-\frac{(f-f_{oc})^2}{2\sigma_{oc}^2}\right)} \qquad (4)$$

where

$$\sigma_{oc}^2 = \frac{\sigma_c^2}{\left(1+\frac{\sigma_c^2}{\sigma_\omega^2}\right)} \quad f_{oc} = \frac{\left(f_c + \frac{\sigma_c^2 f_o}{\sigma_\omega^2}\right)}{\left(1+\frac{\sigma_c^2}{\sigma_\omega^2}\right)}. \qquad (5)$$

In (5), f_o and σ_ω^2 are the peak frequency and bandwidth of the reference power spectrum prior to filtering. After applying the filters, the peak frequencies of the back scattered power spectrum from the reference and the tissue can be related as

$$\left(f_{oc} - \tilde{f}_{oc}''\right) \cong 4 z_T \alpha_o \tilde{\sigma}_{\omega c}^2 + An\tilde{\sigma}_{\omega c}^2 f_{oc} \qquad (6)$$

where A and n are constants related to the frequency dependence of the scattering, z_T is the propagation depth, and α_o is the slope of the total attenuation. For inhomogeneous tissue, α_o is a weighted sum of all of the attenuations along the propagation path. Based on (6), it is possible to determine the total attenuation along the propagation path by applying multiple filters to the backscattered power spectrum from the tissue and the reference (i.e., different f_{oc}) and calculating

$$\xi(f_{oc}) = \frac{\left(f_{oc} - \tilde{f}_{oc}''\right)}{4 z_T \tilde{\sigma}_{\omega c}^2} \cong \alpha_o + \frac{An}{4 z_T} f_{oc} \qquad (7)$$

for each filter. Fitting a line to $\xi(f_{oc})$ versus f_{oc} and finding the intercept will then yield α_o.

III. Simulation Parameters and Results

In order to evaluate the algorithm, computer simulations were performed. In the simulations, a spherically focused ultrasound source exposed an attenuating homogeneous half-space. The source had a focal length of 5 cm, an f-number of 4, a center frequency of 14 MHz, and a -3 dB bandwidth on transmit of 50 %. The sound speed of the half-spaces was 1540 m/s, and the attenuation of the half-spaces was varied from 0.1 dB/cm-MHz to 0.9 dB/cm-MHz in order to assess the dependence of the algorithm on attenuation. The scattering structures within each half-space had Gaussian correlation functions (i.e., form factor of $F_\gamma(f, a_{eff}) = e^{\left(-0.827(ka_{eff})^2\right)}$) with an a_{eff} from 5 to 55 μm and were positioned at a density of 250/mm^3 (~5 scatterers per resolution cell for 14 MHz transducer).

In these initial simulations, a total of 3 Gaussian filtering functions were applied to the power spectra spanning the entire usable frequency range. The center frequencies, f_c, for these filters were determined automatically by the code from

$$\begin{aligned} f_{c1} &= f_{\min} + \frac{f_{\max} - f_{\min}}{4} \\ f_{c2} &= f_{c1} + \frac{f_{\max} - f_{\min}}{4} \\ f_{c3} &= f_{c2} + \frac{f_{\max} - f_{\min}}{4} \end{aligned} \qquad (8)$$

where f_{max} and f_{min} correspond to the largest and smallest frequencies in the -20 dB bandwidth of the received power spectrum. Once the values of f_c were set, the bandwidths of the filters, σ_c^2, were determined by finding the percent bandwidth that resulted in f_{min} corresponding to the smallest -10 dB

frequency for the first filter. All of the filters then used the same percent bandwidth.

The first simulations attempted to find the optimal region of interest size (ROI) in the axial direction. This was done by using a rectangular windowing function to gate the time domain windows about the focus with a length of 2.2 to 8.8 mm. The value of $\mathrm{E}\left[\left|V_{scat}(f)\right|^2\right]$ was then determined by averaging the power spectrum from 100 independent echoes. The accuracy and precision of the total attenuation estimates as a function of window length is shown in Fig. 1.

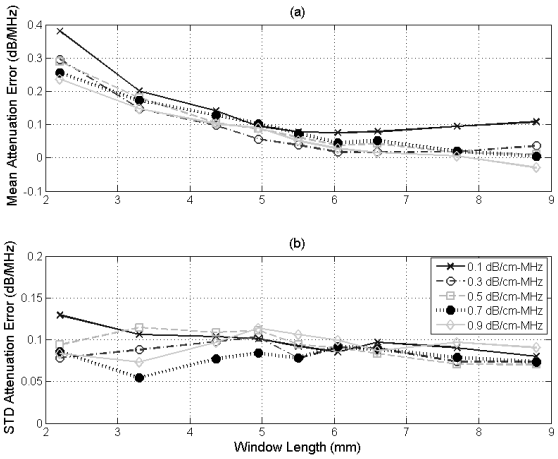

Figure 1. The (a) accuracy and (b) precision of the algorithm in dB/MHz versus window length used to gate the time domain waveforms for half space attenuations of 0.1 to 0.9 dB/cm-MHz for a scatterer size of 25 μm when averaging the power spectrum from 100 independent echoes.

In Fig. 1., the accuracy improves with increasing window length up to a window length of approximately 6 mm while the precision remains relatively constant. Based on these results, we selected a window length of 6.6 mm for the optimal ROI size for our transducer in these simulations.

After determining the optimal ROI size, the dependence on the number of independent echoes was determined by varying the number of echoes from 10 to 100 echoes with the results shown in Fig. 2. When varying the number of echoes, the accuracy of the algorithm is constant while the precision improves as the number of echoes increases. However, the improvement in precision is minimal after about 40 to 50 echoes, therefore 50 echoes was selected as the optimal value in the rest of the simulations.

The performance of the algorithm was then evaluated for varying scatterer sizes. The accuracy and precision of the algorithm for the echoes from the half-spaces with an attenuation of 0.5 dB/cm-MHz and scatterer effective radii from 5 to 55 μm is shown in Fig. 3. The algorithm is able to accurately estimate the total attenuation slope independent of scatterer size. However, there is a slight degradation in the accuracy of the algorithm as the scatterer size increases. This is likely due to neglecting higher order terms in $An\sigma_\omega^2$ which are proportional to scatterer size.

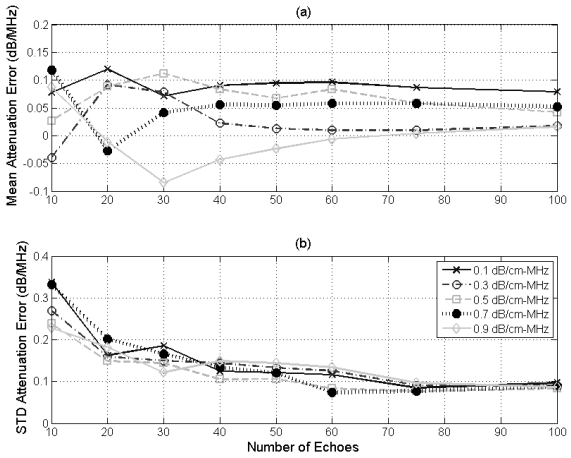

Figure 2. The (a) accuracy and (b) precision of the algorithm in dB/MHz versus the number of independent echoes for half space attenuations of 0.1 to 0.9 dB/cm-MHz for a scatterer size of 25 μm when using a window length of 6.6 mm to gate the time domain waveform.

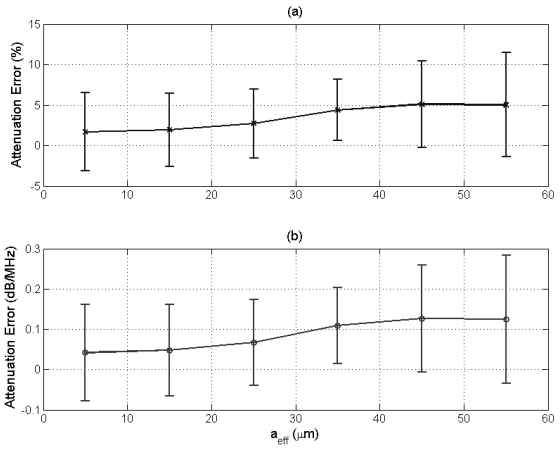

Figure 3. Plot of mean and standard deviation of error in attenuation slope in (a) % and in (b) dB/MHz versus the effective radius of the scatterers in the half-space. The window length used in this simulation was 6.6 mm and 50 independent echoes were used when estimating the power spectra. The error bars correspond to one standard deviation above and below the mean value.

IV. Discussion and Conclusions

In our study, we adapted our previously developed algorithm for implementation using echoes from a single source. Whereas our earlier algorithm required echoes from multiple sources scanning the same tissue region, our new algorithm was able to obtain the same results by applying multiple Gaussian filters to the echo data from a single source. This was the first critical step in extending the algorithm to the clinic. In the future, the algorithm will be extended to array sources as opposed to the single element spherically focused sources used in our simulations in this study.

References

[1] F. L. Lizzi, M. Greenebaum, E. J. Feleppa, M. Elbaum, and D. J. Coleman, "Theoretical framework for spectrum analysis in ultrasonic tissue characterization," *The Journal of the Acoustical Society of America,* vol. 73, pp. 1366-1373, 1983.

[2] M. F. Insana and T. J. Hall, "Parametric ultrasound imaging from backscatter coefficient measurements: Image formation and interpretation," *Ultrason. Imaging,* vol. 12, pp. 245-267, 1990.

[3] M. F. Insana, R. F. Wagner, D. G. Brown, and T. J. Hall, "Describing small-scale structure in random media using pulse-echo ultrasound," *The Journal of the Acoustical Society of America,* vol. 87, pp. 179-192, 1990.

[4] F. L. Lizzi, M. Astor, T. Liu, C. Deng, D. J. Coleman, and R. H. Silverman, "Ultrasonic spectrum analysis for tissue assays and therapy evaluation," *International Journal of Imaging Systems and Technology,* vol. 8, pp. 3-10, 1997.

[5] F. L. Lizzi, M. Astor, A. Kalisz, T. Liu, D. J. Coleman, R. Silverman, R. Ursea, and M. Rondeau, "Ultrasonic spectrum analysis for assays of different scatterer morphologies: Theory and very-high frequenc clinical results.," *Int J Imaging Syst Technol,* vol. 8, pp. 3-10, 1997.

[6] M. L. Oelze, W. D. O'Brien, Jr., J. P. Blue, and J. F. Zachary, "Differentiation and characterization of rat mammary fibroadenomas and 4T1 mouse carcinomas using quantitative ultrasound imaging," *IEEE Transactions on Medical Imaging,* vol. 23, pp. 764-771, 2004.

[7] M. L. Oelze and J. F. Zachary, "Examination of cancer in mouse models using high-frequency quantitative ultrasound," *Ultrasound in Medicine & Biology,* vol. 32, pp. 1639-1648, 2006.

[8] T. A. Bigelow, M. L. Oelze, and W. D. O'Brien, Jr., "Estimation of total attenuation and scatterer size from backscattered ultrasound waveforms," *The Journal of the Acoustical Society of America,* vol. 117, pp. 1431-1439, 2005.

[9] P. He and J. F. Greenleaf, "Application of stochastic analysis to ultrasonic echoes---Estimation of attenuation and tissue heterogeneity from peaks of echo envelope," *The Journal of the Acoustical Society of America,* vol. 79, pp. 526-534, 1986.

[10] H. Tu, J. Zagzebski, and Q. Chen, "Attenuation estimations using envelope echo data: Analysis and simulations," *Ultrasound in Medicine & Biology,* vol. 32, pp. 377-386, 2006.

[11] F. L. Lizzi, J. Driller, B. Lunzer, A. Kalisz, and D. J. Coleman, "Computer model of ultrasonic hyperthermia and ablation for ocular tumors using b-mode data," *Ultrasound in Medicine & Biology,* vol. 18, pp. 59-73, 1992.

[12] D. A. Sidney, "Three-dimensional ultrasound power deposition modeling, thermal field visualization, and clinical integration of hyperthermia therapy." vol. PhD Dissertation Boston, MA.: Massachussetts Institute of Technology, 1997.

[13] H. Kim and T. Varghese, "Attenuation estimation using spectral cross-correlation," *Ultrasonics, Ferroelectrics and Frequency Control, IEEE Transactions on,* vol. 54, pp. 510-519, 2007.

[14] T. A. Bigelow, B. L. McFarlin, W. D. O'Brien Jr, and M. L. Oelze, "In vivo ultrasonic attenuation slope estimates for detecting cervical ripening in rats: Preliminary results," *The Journal of the Acoustical Society of America,* vol. 123, pp. 1794-1800, 2008.

[15] T. A. Bigelow and W. D. O'Brien, Jr., "Signal processing strategies that improve performance and understanding of the quantitative ultrasound SPECTRAL FIT algorithm," *The Journal of the Acoustical Society of America,* vol. 118, pp. 1808-1819, 2005.

[16] T. A. Bigelow and W. D. O'Brien, Jr., "Evaluation of the spectral fit algorithm as functions of frequency range and Dka_{eff}," *IEEE Transactions on Ultrasonics, Ferroelectrics, and Frequency Control,* vol. 52, pp. 2003-2010, November 2005.

[17] T. A. Bigelow, "Ultrasound attenuation estimation using backscattered echoes from multiple sources," *The Journal of the Acoustical Society of America,* vol. 124, pp. 1367-1373, 2008.